# Pseudo-dynamic tests in centrifugal field for structure-foundation-soil systems

**Yoshikazu Takahashi**
*Kyoto University, Kyoto, Japan*

**Masako Kodera**
*Tokyo Electric Power Company, Kawasaki, Japan*

**SUMMARY:**
The pseudo-dynamic test method in centrifugal field is proposed for the soil-foundation-structure interaction problem. The structure part is modelled numerically and the foundation-soil system is modelled and tested in the centrifuge. Since the actuator is attached and controlled at the top of the foundation, the inertia interaction is the main focus in this study. Although this test method is static, the effect of the complex stiffness of the foundation-soil system can be considered by a gyro-mass that generates a reaction force proportional to the relative acceleration. To clarify the effectiveness of the test method, shaking table tests are also conducted and the results of the shake table tests shows a good agreement with that of the pseudo-dynamic tests. However the soil deformation becomes large, the max displacement of the foundation is underestimated. To improve the accuracy of the pseudo-dynamic test, kinematic interaction has to be considered.

*Keywords: pseudo-dynamic test, soil-structure interaction, centrifuge test*

## 1. INTRODUCTION

Soil-foundation-structure interaction (SFSI) has a great effect on the seismic behaviour of structural system. A considerable number of studies have been made on this effect analytically and experimentally.

In analytical approach, FEM and BEM are the powerful methods to consider complex behaviour of SFSI. Penzien-type modelling is often used for SFSI problems and sometimes a simple soil spring is adopted. The key point for analytical approach is how to evaluate the model properties adequately, but it is very difficult to find them and the analytical approach sometimes has the limitation because of the modelling.

In experimental approach, forced vibration test by dynamic actuator, shaking table test and centrifuge test are often conducted for studying SFSI. Tokimatsu studied the effect of inertial and kinematic forces on pile stresses based on full scale shaking table tests in dry and saturated sand. However, conducting site experiments and large scale tests need the big effort and substantial cost. Therefore these test can't be conducted a number of times.

On the other hand, centrifuges enable the small scale tests in geotechnical engineering field and many tests have been conducted. This is because a high gravitation field generated by centrifugal force makes the stress field in a model equal to that in its prototype.

But a model in centrifuge is too small to simulate complicated behaviour of nonlinear structures, i.e. concrete columns. To overcome this difficulty, a pseudo-dynamic test method in centrifugal field is proposed. The pseudo-dynamic test is a hybrid method of the numerical analysis and the physical experiment. To clarify the effectiveness of the test method, shaking table tests are also conducted.

## 2. SFSI AND FREQUENCY-DEPENDENT SOIL SPRING

### 2.1. Structure Foundation Soil Interaction

*2.1.1. Effects of inertial and kinematic interaction*

Frequency-dependent soil spring can represent Load-Displacement relationship at the boundary between the structure and ground. And Foundation input motion can represent the input seismic motion acting on the structure through the Frequency-dependent soil spring. The effect of Frequency-dependent soil spring and Foundation input motion are called Inertial interaction and Kinematic interaction, respectively. The effect of frequency dependence and radiation damping is classified into Inertial interaction. Input loss effect is sorted into Kinematic interaction.

*2.1.2. Frequency-dependent soil spring*

Frequency-dependent soil spring have some characteristics. One is the spring effect which makes resistance force proportional to the deformation, and another is the dashpot effect which makes resistance force proportional to the rate of deformation. The radiation damping is representative of the latter effect. Moreover, Frequency-dependent soil spring have the added mass effect which is caused by the soil vibration following the foundation motion.

The characteristics of Frequency-dependent soil spring $K_g$ is denoted by the following formula,

$$K_g(\omega) = K_f(\omega) - \omega^2 \bar{M} + j\omega C_f(\omega) \tag{2.1}$$

$\bar{M}$ is the added mass. ω is angular frequency and j is imaginary unit. Then $K_f \cdot C_f$ are the constant numbers corresponding to stiffness and damping. Frequency-dependent soil spring can be expressed in complex form.

*2.1.3. Foundation input motion*

Generally, seismic motion on the foundation is smaller than that on the free field surface. The phenomenon is called input loss effect. It is caused by the embedded foundation and the various angle of seismic wave. In aseismic design, the surface motion of the free field and the bottom motion of the foundation are usually used as input motion.

### 2.2. Time Domain Analysis with the Frequency-Dependent Soil Spring.

*2.2.1. Causality*

It is important to consider frequency-dependent soil spring to study SFSI analytically. Ordinarily, using frequency-dependent spring need to analyze in the frequency domain. It is impossible to analyze nonlinear problem. So, the special analysis method is needed to analyze in the time domain.

Causality is a key point of analysis in time domain with frequency-dependent spring. Considering 1 degree freedom of system which consists of a spring, a mass and a dashpot, the motion equation is

$$m\ddot{x}(t) + c\dot{x}(t) + r(t) = -m\ddot{u}_g(t) \tag{2.2}$$

m and c is mass and damping. r is restoring force, $\ddot{u}_g$ is input acceleration. In frequency domain,

$$-\omega^2 m x(\omega) + j\omega c x(\omega) + r(\omega) = \omega^2 m u_g(\omega) \tag{2.3}$$

If c and r are the function of $\omega$, these are divided into constant term and dependent term on $\omega$.

$$c = c_0 + c_\omega(\omega)\ , \quad r(\omega) = \{1 + R_\omega(\omega)\} r_0(\omega) \tag{2.4}$$

By substituting Eqn.2.4 into Eqn.2.3,

$$-\omega^2 mx(\omega) + j\omega c_0 x(\omega) + r_0(\omega) = \omega^2 m u_g(\omega) - \left\{R_\omega(\omega) + j\omega c_\omega(\omega)\frac{x(\omega)}{r_0(\omega)}\right\} r_0(\omega) \tag{2.5}$$

$k^*(\omega)$ is defined by $k^*(\omega) = R_\omega(\omega) + j\omega c_\omega(\omega)\frac{x(\omega)}{r_0(\omega)}$ Then Eqn.2.5 become the following equation in time domain which form is Eqn.2.2 added convolution term.

$$m\ddot{x}(t) + c_0\dot{x}(t) + r_0(t) = -m\ddot{u}_g(t) - \int_{-\infty}^{\infty} k^*(t-\tau) r_0(\tau) d\tau \tag{2.6}$$

$k^*(t)$ is inverse Fourier transform of $k^*(\omega)$. However, Eqn.2.6 doesn't satisfy the causality, so the current state depended on the future state. This can't represent the actual phenomenon. The integral interval of convolution term has to be changed into 0-t to satisfy the causality.

$$m\ddot{x}(t) + c_0\dot{x}(t) + r_0(t) = -m\ddot{u}_g(t) - \int_{0}^{t} k^*(t-\tau) r_0(\tau) d\tau \tag{2.7}$$

Furthermore the real and imaginary parts of $k^*(\omega)$ have to be Hilbert transform pair.

*2.2.2. Saitoh's method*

Saitoh propose the method which can consider frequency-dependent spring using the normal algorism of the seismic response analysis. The characteristic of Saitoh's method is the gyromass which generates a reaction force proportional to the relative acceleration. The base system (Upper side of Figure 2.1) is consists of the spring $K_f$, the dashpot $C_f$ and the gyromass $\overline{M}_b$. The complex stiffness of base system is as follows.

$$K_f - \omega^2 M_b + j\omega C_f \tag{2.8}$$

Eqn.2.8 represent the added mass effect. And the core system (Lower side of Figure 2.1) also consist of the spring $k_c$, the dashpot $c_c$ and the gyromass $\overline{m}_c$. The complex stiffness of core system is as follows.

$$\frac{\overline{m}_c\omega^2\left(\frac{\overline{m}_c\omega^2}{k_c} - \frac{c_c^2\omega^2}{k_c^2} - 1\right)}{\left(1 - \frac{\overline{m}_c\omega^2}{k_c}\right)^2 + \frac{c_c^2\omega^2}{k_c^2}} + j\omega\frac{\overline{m}_c\omega^2\frac{\overline{m}_c c_c\omega^2}{k_c}}{\left(1 - \frac{\overline{m}_c\omega^2}{k_c}\right)^2 + \frac{c_c^2\omega^2}{k_c^2}} \tag{2.9}$$

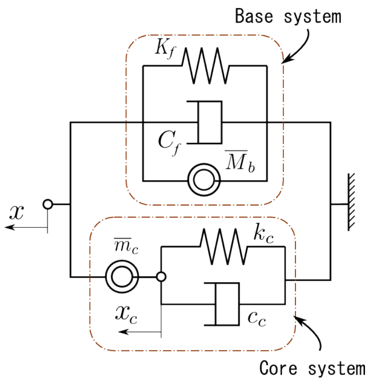


**Figure 2.1** The frequency-dependent spring (Saitoh's metohd)

Connecting the base system and the core system in parallel, the complex stiffness of Figure 2.1 can described Eqn.2.10 from Eqn.2.8 and Eqn.2.9.

$$K_f - \omega^2 \bar{M}_b \frac{\bar{m}_c \omega^2 \left( \frac{\bar{m}_c \omega^2}{k_c} - \frac{c_c^2 \omega^2}{k_c^2} - 1 \right)}{\left(1 - \frac{\bar{m}_c \omega^2}{k_c}\right)^2 + \frac{c_c^2 \omega^2}{k_c^2}} + j\omega \left\{ C_f + \frac{\bar{m}_c \omega^2 \frac{\bar{m}_c c_c \omega^2}{k_c}}{\left(1 - \frac{\bar{m}_c \omega^2}{k_c}\right)^2 + \frac{c_c^2 \omega^2}{k_c^2}} \right\} \tag{2.10}$$

The arbitrary complex stiffness can described by determine $\bar{M}_b$, $k_c$, $c_c$ and $\bar{m}_c$, the parameters of Eqn.2.10. The motion equation of Figure 2.1 is as follows.

$$\begin{bmatrix} M + \bar{M}_b & -\bar{m}_c \\ -\bar{m}_c & \bar{m}_c \end{bmatrix} \begin{Bmatrix} \ddot{x} \\ \ddot{x}_c \end{Bmatrix} + \begin{bmatrix} C_f & 0 \\ 0 & c_c \end{bmatrix} \begin{Bmatrix} \dot{x} \\ \dot{x}_c \end{Bmatrix} + \begin{bmatrix} K_f & 0 \\ 0 & k_c \end{bmatrix} \begin{Bmatrix} x \\ x_c \end{Bmatrix} = -\begin{Bmatrix} M \\ 0 \end{Bmatrix} \ddot{u}_g \tag{2.11}$$

Eqn.2.11 can be solved by numerical integration method such as Newmark method. Only changing [M], [K], [C] matrix, Eqn.2.11 can be incorporated into exiting experience system.

However, it is impossible to consider the causality. The complex stiffness satisfying the causality is needed by another method and the parameters are determined to fit the complex stiffness.

## 3. APPLICABILITY OF PSEUDO-DYNAMIC TEST TO SFSI PROBLEMS

### 3.1. Application to Inertial Interaction

*3.1.1. Frequency-dependent soil spring*

Studying SFSI, the soil spring between the ground and foundation needs to depend on frequency. The frequency dependency is considered automatically in the hybrid experience with a dynamic actuator. However, the normal algorism of the pseudo-dynamic test with a static actuator doesn't have frequency dependency. The analysis algorism of the pseudo-dynamic test has to be change to calculate frequency-dependent soil spring in time domain.

Toki conducted pseudo-dynamic test for the soil-foundation interaction by full scale model. The complex stiffness was presumed from the result of the dynamic test conducted before hand. The system of this pseudo dynamic test took in the complex stiffness and it enabled the frequency dependence is take into account. The motion equation of the system is as follows.

$$m\ddot{x}(t) + c_0 \dot{x}(t) + r_0(t) = -m\ddot{u}_g(t) - \int_0^t \frac{2\alpha}{\pi} \frac{\sin \omega_0 (t-\tau)}{t-\tau} \ddot{r}_0(\tau) d\tau \tag{3.1}$$

*3.1.2. Interaction by the structure inertial force*

Applying the load to the foundation with the actuator, the soil deformation by the structure inertial force can be simulated. Considering sway-rocking model, more than one actuator is needed to imitate this phenomenon.

Interaction by the structure inertial force is easily considered in pseudo-dynamic test in centrifugal field. The system of pseudo-dynamic test is constructed in the centrifuge test by modelling structures numerically. This method can consider the nonlinear behaviour of soil and structures in small model experiment.

### 3.2. Application to Kinematic Interaction

*3.2.1. Foundation input motion*

The input loss effect can be simulated theologically by setting the foundation-soil model on shaking table. This experiment needs dynamic actuators. Using both the shaking table and dynamic actuators in hybrid experience have studied before, but it will become very large system.

*3.2.2. Interaction by the soil deformation*

The effect of soil deformation to the structure can't be estimated by using the rigid box because the soil hardly moves in pseudo-dynamic test. But using a shear box can solve this problem. The soil deformation can cause by applying the load from the outside of the shear box with multi-actuator.
This system will grow in size, so centrifuge test which is suitable for small scale model is predictably effective for this system.

### 3.3. Similitude

The similitudes of centrifugal field and pseudo-dynamic test are corresponding. Centrifugal force controlled gravitational acceleration to satisfy similitude. In pseudo-dynamic testing, physical quantities such as mass and time are used only in numerical calculations, because only displacement x and restoring force R are applied and measured. The test itself is carried out in pseudo time. Table 3.1 shows each similitude.

**Table 3.1** Similitude prototype/model scale (Bold text indicate precondition)

| | Centrifugal field | Pseudo-dynamic Test |
|---|---|---|
| Length | **n** | **n** |
| Mass density | **1** | **1** |
| Mass | $n^3$ | $n^3$ |
| Stress | **1** | **1**<br>adding external axial force by actuators |
| Acceleration | 1/n | 1/n |
| Time | n | n |

## 4. EXPERIMENTAL SETUP

### 4.1. Objective System

The objective system of this study is shown in Figure 4.1(a). Supposing the soil behave nonlinearly, the foundation part (footing) is pushed by the static actuator. It means the target is inertial interaction.

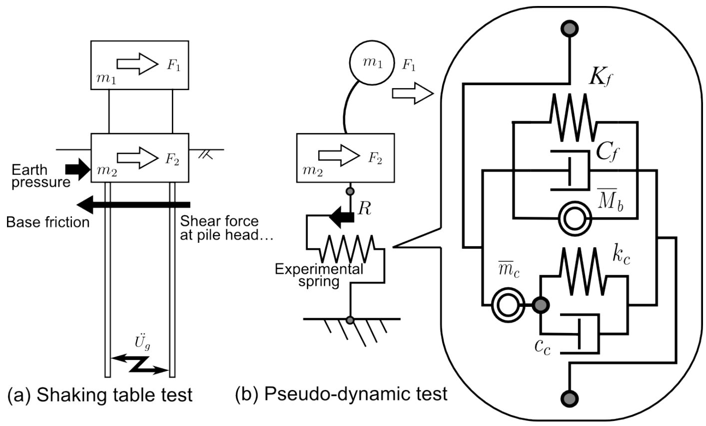


**Figure 4.1** The objective system and numerical model

### 4.2. Experimental Setup

The tests are conducted in 40G centrifugal acceleration at the Disaster Prevention Research Institute, Kyoto University. The soil box is rigid and the size is. 450mm x 150mm x 300mm (length x width x height). The soil is silica sand and the relative density is 60-67%. The foundation model consists of a footing and 2 x 2 piles. The pile is square pole with the dimensions of 10 mm (width). 7 pairs of strain gauge are put in one pile. To prevent a rocking motion of the foundation, the pile heads and pile ends are fixed. The soil and foundation model are common in the shaking table and the pseudo-dynamic tests.

### 4.3. Shaking Table Test

To compare the pseudo-dynamic test, the shaking table test in centrifugal field is conducted. The experimental model of the shaking table test is shown in Figure 4.2. The superstructure consists of a brass mass and flat springs made of phosphor bronze and connected to the footing by 4 flat springs rigidly. Therefore rocking motion is prevented and sway motion became dominant. Flat springs have 2 pairs of strain gauge. The input motion is JR Takatori record (EW component) which amplitude and time are set to 4mm, 1/40 respectively. Figure 4.3 shows the acceleration waveform measured in the shaking table test.

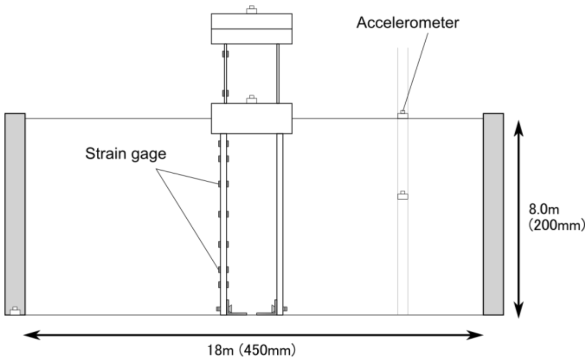


**Figure 4.2** Model of the shaking table test

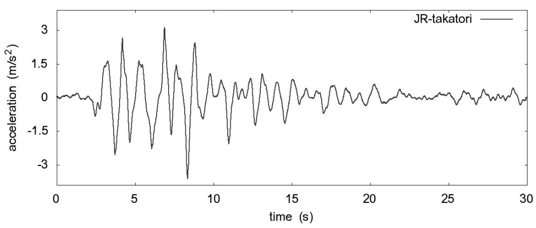


**Figure 4.3** Input accerelation

### 4.4. Pseudo-Dynamic Test

The numerical model consists of 2 node, superstructure and footing. The model image is shows in Figure 4.1(b). $F_s$ and $F_f$ are inertial force of superstructure and footing. $F_s + F_f$ is equal to restoring force $R_f$. $R_f$ include all force acting on the footing such as the earth pressure, the shear force at the pile head and the base friction.

The standard motion equation of pseudo-dynamic test is as follows.

$$\begin{bmatrix} M_s & 0 \\ 0 & M_f \end{bmatrix} \begin{Bmatrix} \ddot{x}_s \\ \ddot{x}_f \end{Bmatrix} + \begin{bmatrix} C_s & -C_s \\ -C_s & C_s + C_f \end{bmatrix} \begin{Bmatrix} \dot{x}_s \\ \dot{x}_f \end{Bmatrix} + \begin{Bmatrix} R_s \\ R_f \end{Bmatrix} = -\begin{Bmatrix} M_s \\ M_f \end{Bmatrix} \ddot{u}_g \tag{4.1}$$

$M$ is mass and C is damping coefficient. $x$ is displacement and $u_g$ is horizontal displacement of ground. Subscripts "s" denote the superstructure and "f" denote footing. Restoring force $R_f(t)$ is measured in the experiment. Substituting $R_f(t)$ into Eqn.4.1, the next step displacement $\{x(t+1)\}$ is calculated. Considering similitude, input $x_f(t+1)$ in the experiment and the restoring force $R_f(t)$ is measured.

To consider frequency dependency, Eqn.4.1change into the following equation by the Saitoh's method and the numerical model is Figure.4.1(b).

$$\begin{bmatrix} M_s & 0 & 0 \\ 0 & M_f + \bar{M}_b & -\bar{m}_c \\ 0 & -\bar{m}_c & \bar{m}_c \end{bmatrix} \begin{Bmatrix} \ddot{x}_s \\ \ddot{x}_f \\ \ddot{x}_c \end{Bmatrix} + \begin{bmatrix} C_s & -C_s & 0 \\ -C_s & C_s + C_f & 0 \\ 0 & 0 & c_c \end{bmatrix} \begin{Bmatrix} \dot{x}_s \\ \dot{x}_f \\ \dot{x}_c \end{Bmatrix} + \begin{Bmatrix} R_s \\ R_f \\ k_c x_c \end{Bmatrix} = -\begin{Bmatrix} M_s \\ M_f \\ 0 \end{Bmatrix} \ddot{u}_g \tag{4.2}$$

Eqn.4.2 is the basic equation of the pseudo-dynamic test with frequency-dependent soil spring. The system of pseudo-dynamic test is used OpenFresco for experimental setup and control and OpenSees for earthquake simulation. These are Software Framework for hybrid simulation of the numerical analysis and the physical experiment.

Figure 4.4 shows the model of the pseudo-dynamic test. The actuator which consists of stepping motor and ball screw pushes on the top of the foundation part. A load cell is used for recording the restoring force and a digital laser displacement sensor improves the precision of measurement. A rigid block is added on the footing to connect the actuator. The calculated displacement applied to the footing by the horizontal movement of the actuator.

### 4.5. Experimental Case

The pseudo-dynamic test conducted to simulate the shaking table test. Therefore the superstructure is assumed to linear. The stiffness of superstructure fit the model of the shaking table test. Input motion is the recorded acceleration at ground surface or the shaking table of the shaking table test. Table 4.1 shows the parameter of both of the experiments. The 2 case conducted, changing the superstructure mass. Case1 don't use frequency-dependent soil spring. Figure 4.5 shows the complex stiffness of frequency-dependent soil spring in Case2.

**Table 4.1** The parameter of the shaking table test and the pseudo-dynamic test

(a) The shaking table test

| | | | | Case1 | Case2 |
|---|---|---|---|---|---|
| superstructure | mass | $M_s$ | t | 54.7 | 27.2 |
| | stiffness | $K_s$ | kN/m | $5.2\times10^3$ | $5.2\times10^3$ |
| footing | mass | $M_f$ | t | 49.0 | 49.0 |

(b) The pseudo-dynamic test

| | | | | Case1 | Case2 |
|---|---|---|---|---|---|
| superstructure | mass | $M_s$ | t | 54.7 | 27.2 |
| | stiffness | $K_s$ | kN/m | $5.2\times10^3$ | $5.2\times10^3$ |
| | damping | $C_s$ | kNs$^2$/m | 0 | 0 |
| foundation | mass | $M_f$ | t | 49.0 | 49.0 |
| | Base system | $K_f$ | kN/m | $5.8\times10^7$ | $5.8\times10^7$ |
| | | $C_f$ | kNs$^2$/m | 17.3 | 13.4 |
| | | $\bar{M}_b$ | t | 5.15 | $3.2\times10^{-4}$ |
| | Core system | $m_c$ | t | 0 | 10.9 |
| | | $k_c$ | kN/m | 0 | $4.8\times10^4$ |
| | | $c_c$ | kNs$^2$/m | 0 | $2.0\times10^3$ |
| Input acceleration | | | | Shaking table | Ground surface |

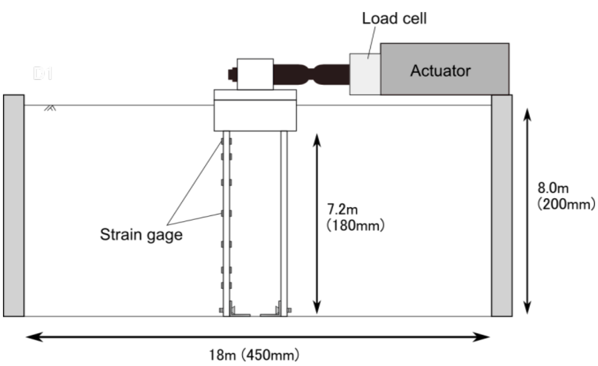


**Figure 4.4** Model of the pseudo-dynamic test

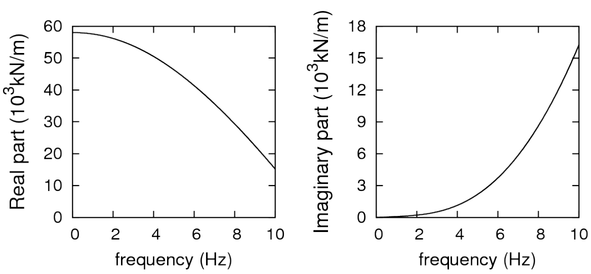


**Figure 4.5** The complex stiffness of frequency-dependent soil spring in Case2

## 5. THE RESULT OF TESTS

### 5.1. Numerical Integration Method of Pseudo-Dynamic Test

In Pseudo-dynamic test, the displacement errors such as undershoot errors excite the highest mode of the system, and the response tends to have high-frequency noise. Therefore, $\alpha$-OS method is usually used because of solution stability and residual control.

On the other hand, the frequency become higher, the stiffness of the frequency-dependent soil spring is smaller and the damping is bigger. About damping, $\alpha$-OS method and the frequency-dependent soil spring have same characteristic. For SFSI problem, $\alpha$-OS method isn't appropriate because the effect of frequency-dependent soil spring is indistinguishable from that of $\alpha$-OS method.

Therefore, Explicit Newmark method is used. Explicit Newmark method has no numerical damping, but it is conditional stability. It needs enough small time step compared the natural period of the objective system. Too small displacement have to be controlled by too small time step, so Explicit Newmark method is unsuitable for large degree of freedom system. It is no matter in this study because degree of freedom is only 2.

### 5.2. The Effect of Frequency-Dependent Soil Spring

Figure 5.1 shows the comparison of the pseudo-dynamic test with non-frequency-dependent soil spring and frequency-dependent soil spring. The frequency higher than 6Hz attenuate and this is the effect of the frequency-dependent soil spring. The added mass effect can't find from this result. The reason is the soil nonlinearity is very strong and added mass effect is too small compared nonlinearity.

The effect of frequency-dependent soil spring is found only the noise region of control error. Accordingly the objective problem is less influenced by frequency-dependency.

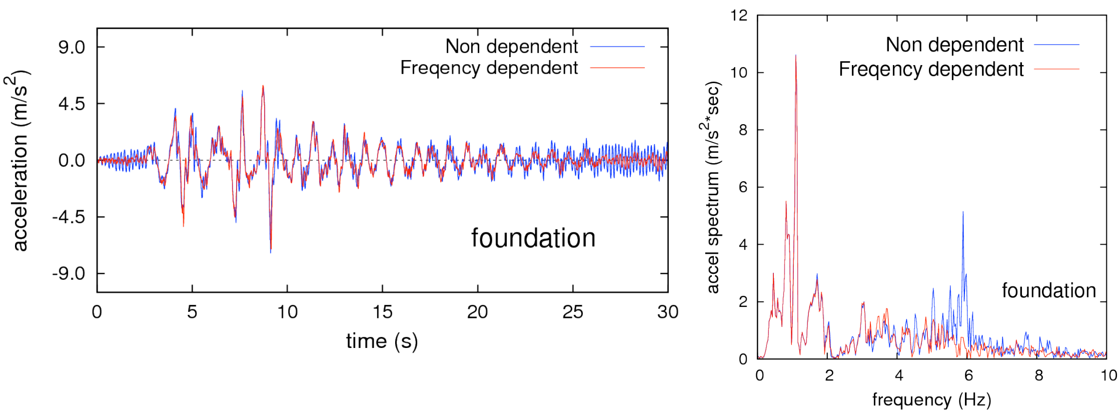


**Figure 5.1** The effect of frequency-dependent soil spring (Case2)

### 5.3. Comparison with the Shaking Table Test.

Figure 5.2 shows the acceleration time history. The amplifications and phase of Case2 are in good agreement about the superstructure and footing. The acceleration of pseudo-dynamic test in Case1 is smaller than that of shaking table test. One possible reason may be that the input motion is the recorded acceleration at the shaking table test. The real input is larger than the input acceleration and the response become smaller. But the phase and the wave form are very similar.

Figure 5.3 shows the displacement time history. Case1 have the same tendency as the acceleration. Even the residual displacement of pseudo-dynamic test in Case2 fit closely with that of the shaking table test. Figure 5.4 shows hysteresis loop of footing in Case2. Initial stiffness, equivalent stiffness and eternal shape agree well. Figure 5.5 shows the bending moment distribution of pile between 7.264

– 7.648sec in Case2. The inflexion point and the maximum value of each depth are exactly similar. In actual experiment time, shaking table test takes only 0.75 seconds while pseudo-dynamic test takes 9000 seconds. In spite of the time scale difference, pseudo-dynamic test can simulate the shaking table test very well.

However, About Case2, Figure 5.3 and 5.4 indicate the pseudo-dynamic test underestimate the max displacement response. The force can simulate very well because of the acceleration coincidence. The difference is likely to be due to the external factor which can't be considered in the motion equation Eqn.4.2. The external factor is thought that the pseudo-dynamic test doesn't reflect large soil deformation. Figure 5.6 is the picture at the end of pseudo-dynamic test. The soil of the footing falls in. Because of static experiment, the inertial force can't act on the soil and soil deformation is limited. All of the soil in the box deformed in the shaking tale test, this difference appears as max response difference.

## 6. CONCLUSION

In the present study, the following may be concluded:

- The frequency-dependent spring in time domain can be unified description.
- The frequency-dependent spring is mounted for OpenFresco by using gyromass.
- The pseudo-dynamic test can simulate the shaking table test very well.
- By using frequency-dependent soil spring, the pseudo-dynamic test precisely reflect the damping property. Experimental error can be control by high frequency attenuation.
- The analysis is needed to determine the characteristic of frequency-dependent soil spring.
- The large soil deformation can't be considered in the present pseudo-dynamic test. The new system is needed to apply load directly to not only structure model but also soil model.

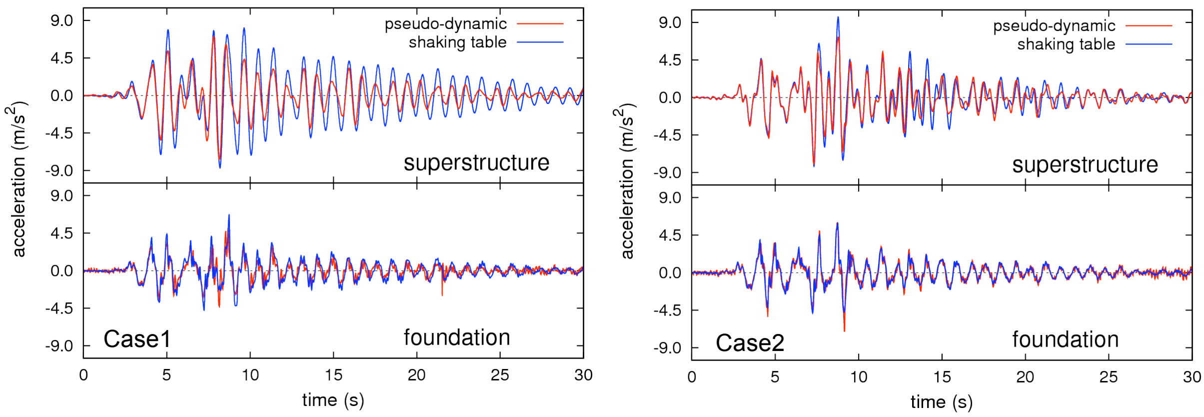


**Figure 5.2** Acceleration time history (Case1 & Case2)

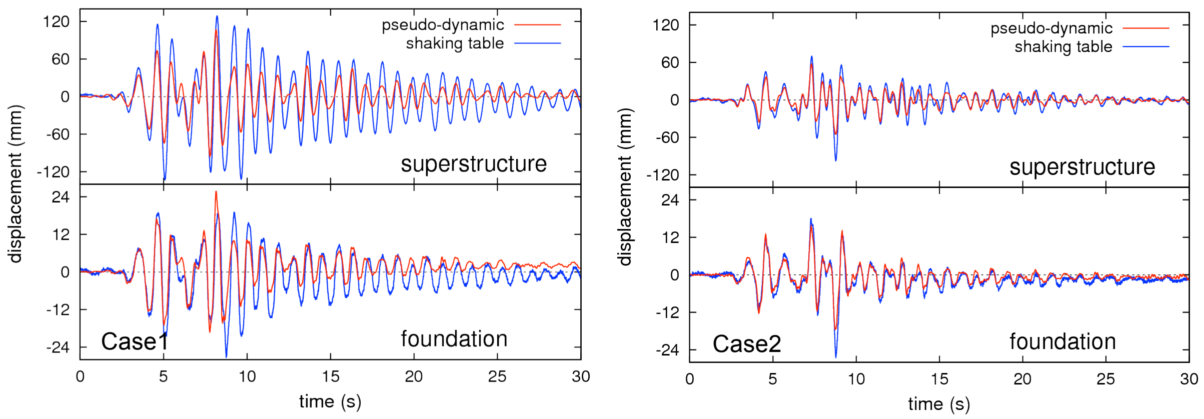


**Figure 5.3** Displacement time history (Case1 & Case2)

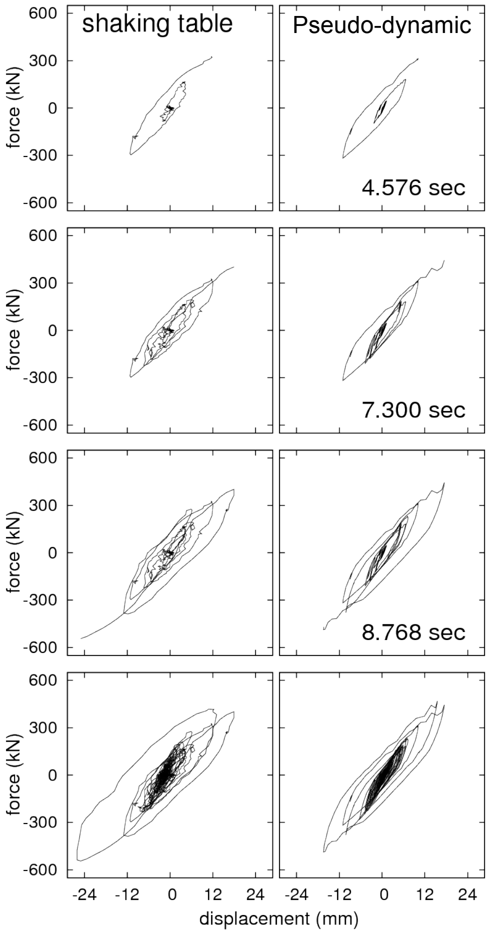


**Figure 5.4** The hysteresis loop of the footing (Case2)

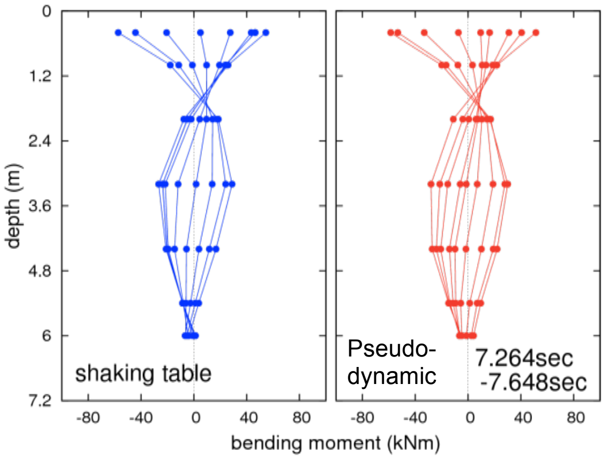


**Figure 5.5** The bending moment distribution (Case2)

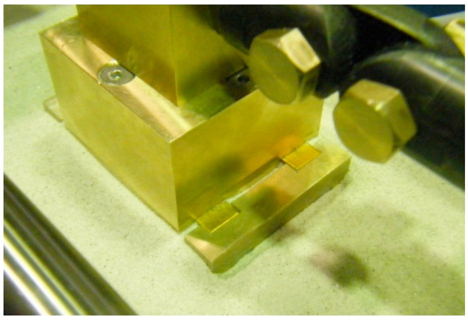

**Figure 5.6** The picture of the end of pseudo-dynamic test

**ACKNOWLEDGEMENT**

This research was supported by Ministry of Education, Culture, Sports, Science and Technology (MEXT). (Grant-in-Aid for Young Scientists (S)19676004, representative : Yoshikazu TAKAHASHI)

**REFERENCES**

Tokimatsua, K., Suzukia, K. and Sato, M. (2005). Effects of inertial and kinematic interaction on seismic behavior of pile with embedded foundation. *Soil Dynamics and Earthquake Engineering* **25**, 753–762

Toki, K., Sato, T., Kiyono, J., Garmroudi, N.K., Emi, S. and Yoshikawa, M. (1990). Hybrid experiments on non-linear earthquake-induced soil-structure interaction. *Earthquake Engineering & Structural Dynamics* **vol 19 issue 5**, 631-787

Saitoh, M. (2007). Simple model of frequency-dependent impedance functions in soil-structure interaction using frequency-independent elements. *Journal of Engineering Mechanics*.**vol 133 issue 10**, 0733-9399

Fenves, G.L., McKenna, F., Scott, M.H. and Takahashi, Y. (2004). An object-oriented software environment for collaborative network simulation, *Proc. of 13th World Conference on Earthquake Engineering*, Paper No. 1492.

Takahashi. Y. and Fenves, G.L. (2006). Software frameword for distributed experimental – computational simulation for structural systems, *Earthquake Engineering & Structural Dynamics*, **Vol. 20, No.2**, 189-206.

Takahashi, Y. and Kodera. M. (2010). Application of pseudo-dynamic test method in centrifugal field for soil-foundation-structure interaction, *Journal of Structural Engineering, JSCE*, **Vol. 56A**, 334-341 , (in Japanese).